

Supporting Information

“Head-to-head” Double-Hamburger-Like Structure of Di-Ruthenated d(GpG) Adducts of Mono-Functional Ru-Arene Anticancer Complex

Hongk-Ke Liu,^{a*} Hana Kostrhunova,^b Abraha Habtemariam,^c Yaqiong Kong,^a Robert J. Deeth,^c Viktor Brabec,^{b*} Peter J. Sadler^{c*}

^a Jiangsu Collaborative Innovation Center of Biomedical Functional Materials, Jiangsu Key Laboratory of Biofunctional Materials, College of Chemistry and Materials Science, Nanjing Normal University, Nanjing 210046, China, ^b Institute of Biophysics, Academy of Sciences of the Czech Republic, v.v.i., Kralovopolska 135, 61265 Brno, Czech Republic and ^c Department of Chemistry, University of Warwick, Gibbet Hill Road, Coventry CV4 7AL, UK.

Contents

Methods

S1. HPLC and ESI-MS characterization of products of d(GpG) + 1.

S2. Details of NMR analysis

Procedures for assignment of conformers.

Guanine bases Ru₂-GpG.

Determination of binding sites.

Bound fragments **1'a-1'd**.

3'-G and 5'-G bases in Ru₂-GpG

Connectivities between d(GpG) and bound fragments **1'a-1'd**

Table S1. Chemical shifts of en-NH protons of **1'** in the various Ru-arene adducts.

Table S2. Negative ions detected by HPLC-ESI-MS for reaction of [η^6 -biphenyl]RuCl(en)]⁺ (**1**) with d(GpG).

Table S3. Intramolecular NOEs between protons of **1'c** and **1'd** and d(GpG) in conformer **II** (minor).

Table S4. Intramolecular NOEs and distances in model **A** (see Fig. 5A-B) between arene protons of **1'a** and **1'b** in major conformer **I**.

Table S5. Distances between protons of d(GpG) and **1'a** or **1'b** in model **A**.

Table S6. Distances between protons of d(GpG) and **1'c** or **1'd** in model **C** (Fig. 5D).

Figure S1. 600 MHz ¹H NMR spectra of the HPLC-separated di-ruthenated d(GpG) adducts [Ru₂-d(GpG)] in both 100% D₂O (A) and 90% H₂O/10% D₂O solutions (B) at 283 K, 2.34 mM in 0.1 M NaClO₄, pH 7.0.

Assignments of proton resonances for both d(GpG) and **1'a-1'd**, (**1'a-1'd** are the bound fragment **1'**, $\{(\eta^6\text{-biphenyl})\text{Ru}(\text{en})\}^{2+}$), are indicated. The assignments of peaks for bases 5'-**G(I)** and 3'-**G(I)** (major conformer **I**), 5'-**G(II)** and 3'-**G(II)**(minor conformer **II**), bound fragments **1'a** to **1'd** are based on 2D DQF-COSY and NOESY experiments (shown in Figures 3 and 4, see also Tables 1, 2 and 3).

Figure S2. 2D [^1H , ^{15}N] HSQC NMR spectra of di-ruthenated $[\text{Ru}_2\text{-d(GpG)}]$ (2.34 mM, 0.1 M NaClO_4 at 298 K, pH 7.0) in 90% $\text{H}_2\text{O}/10\%$ D_2O . Peaks at 6.55/-28.62 and 6.40/-28.62 ppm are assignable to en-NHu resonances, at 4.32/-28.62 ppm to en-NHd resonances of $[\text{Ru}_2\text{-d(GpG)}]$ ($\text{Ru} = \{(\eta^6\text{-biphenyl})\text{Ru}(\text{en})\}^{2+}$ (**1'**). For atom labels, see Figure 1.

Figure S3. 1D ^{31}P NMR spectrum of di-ruthenated d(GpG) adduct at 298 K in 10% $\text{D}_2\text{O}/90\%$ H_2O , showing two ^{31}P peaks at -5.83 (a) and -4.74 ppm (b). For atom and base labels, see Figure 1 and Table 1.

Figure S4. 2D [^1H , ^{31}P] HSQC NMR spectrum of $\text{Ru}_2\text{-d(GpG)}$ in 90% $\text{H}_2\text{O}/10\%$ D_2O at 298 K. The peak at 4.23/-5.83 ppm is assignable to the 5'-**G(I)**H4'/5'-**G(I)**- ^{31}P connectivity. For atom labels, see Figure 1 and Scheme 1.

Figure S5. Autoradiogram of the ligation products of double-stranded oligonucleotides TGGT (19-23) nonmodified or containing two monofunctional adducts of Ru-biphenyl. The ligation products were separated on an 8% PAA gel. Lanes: Control, nonmodified duplexes; $\text{Ru}_2\text{-GpG}$, duplexes containing two adjacent Ru-biphenyl adducts.

Figure S6. Sequences of the synthetic oligodeoxyribonucleotide duplexes used in this study and their abbreviations.

Figure S7. Plots showing the relative mobility K versus sequence length for the oligomers (TGGT)/(ACCA) (19-23) containing Ru-biphenyl adducts.

S1. HPLC and ESI-MS characterization of products of d(GpG) + **1**

Aqueous solutions of **1** were incubated with d(GpG) at Ru : d(GpG) molar ratios of 1 : 1, 2 : 1 and 5 : 1 in the dark, and then analyzed by HPLC. New peaks were observed for each reaction (Figure 2 and Table S2), and adducts associated with them were identified subsequently by ESI-MS. The peaks for the observed ions are listed in Table S2. Reaction at Ru : d(GpG) molar ratios of 1 : 1 or 2 : 1 resulted in a di-ruthenated product and a mono-ruthenated product together with unreacted **1**-Cl and **1**-H₂O. Reaction at a Ru : d(GpG) molar ratio of 5 : 1, gave one di-ruthenated product and a small amount of mono-ruthenated product together with unreacted **1**-Cl and **1**-H₂O. The HPLC peak for the major di-ruthenated adduct was collected, desalted and re-dissolved in 90% H₂O/10% D₂O or 100% D₂O for 1D and 2D NMR studies (see Figure 2C). This sample was rechecked by HPLC under the same conditions and there was only one peak corresponding to the di-ruthenated adduct.

S2. Details of NMR analysis

Procedures for assignment of conformers. Assignments of the ¹H NMR peaks for the di-ruthenated d(GpG) adduct was made on the basis of established methods,¹⁻³ and detailed information about how to make the assignments were as follow. The H8, H1', H2'' and H2', H3', H4', H5'' and H5' resonances of ruthenated guanine bases were assigned from DQF-COSY and NOESY experiments. The assignments of Ho', Hp', Hm' protons (ring B), Ho, Hp and Hm protons (ring A) and **1'**-en-NH₂ (NHu and NHd, see Figure 1 for labelling) resonances of {(η⁶-biphenyl)Ru(en)}²⁺ (**1'**) were achieved by 2D DQF-COSY and 2D NOESY spectra in both 90% H₂O/10% D₂O and 100% D₂O solutions (Figure S2). The en-NHu and en-NHd protons of bound fragments **1'a-1'd** (Figures 1, S1, S2 and Tables 2 and S1) were assigned from the 1D and 2D NOESY spectra in 90% H₂O/10% D₂O and 100% D₂O solutions. The assignments of Hm and Hp resonances of **1'** were also achieved by correlations to the **1'**-en-NHu resonances in [¹H, ¹H] NOESY NMR data. The two conformers **I** (major) and **II** (minor) of di-ruthenated adduct Ru₂-GpG were assigned by the NOESY connectivities between protons of 5'-G(**I**) 3'-G(**I**), 5'-G(**II**) and 3'-G(**II**) and bound fragments **1'a-1'd**.

Weak COSY cross-peaks were observed among Ho' Hp' and Hm' resonances, and also for Ho, Hp and Hm protons. Notable NOESY cross-peaks were observed between Ho' and Ho protons on the same biphenyl ligand in each bound fragment.

COSY and NOESY connectivities were detected between resonances at 7.40 and 7.22 ppm, and among resonances at 6.25, 6.39 and 5.68 ppm, and a notable NOESY cross-peak was observed between resonances at 7.40 and 6.25 ppm. These peaks are reasonably assigned as Ho', Hp' and Hm', Ho, Hp, Hm protons of bound fragment **1'a**. Similarly, resonances at 7.44, 7.27, 6.38 and 5.68 ppm, at 7.44, 7.27, 6.30, 6.45 and 5.68 ppm, or at 7.80, 7.58, 7.62, 6.13, 6.11 and 5.61 ppm are assigned as Ho', Hp' and Hm', Ho, Hp or Hm protons of bound fragments **1'b**, **1'c** or **1'd**.

The most intense H8 signal (8.22 ppm) showed NOE cross-peaks to signals at 2.52, 5.99 and 4.23 ppm. An NOE and COSY cross-peaks between the signal at 2.52 ppm and a signal at 5.99 ppm was also found (Figures 3-4, Table 1). The signal at 2.52 ppm showed NOE and COSY cross-peaks to a resonance at 2.75 ppm, and NOE cross-peaks to signals at 4.87, 4.23 and 3.77 ppm. These two signals (at 4.23 and 3.77 ppm) were connected in the NOESY and COSY spectra. The signal at 5.99 ppm showed NOE and COSY cross-peaks to a resonance at 2.52 ppm, and NOE cross-peaks to signals at 4.87, 4.23 and 3.77 ppm. On the basis of these observations and the chemical shifts of these resonances, the signals at 5.93, 2.75, 2.52, 4.87, 4.23 and 3.77 ppm were assigned to H1', H2', H2'', H3', H4' and H5'/H5'' resonances of 5'-G of conformer **I**, respectively (Figures S1-S2, Table 1).

The second most intense H8 signal (8.45 ppm) showed NOE cross-peaks to signals at 2.48 and 6.12 ppm (Figures 3-4, Table 1). An NOE and COSY cross-peaks between the signal at 2.48 ppm and a signal at 6.12 ppm was also found. The signal at 2.48 ppm showed NOE cross-peaks to signals at 2.78, 4.70 and 4.19 ppm. The signal at 6.12 ppm showed NOE and COSY cross-peaks to a resonance at 2.48 ppm, and NOE cross-peaks to signals at 4.27 ppm. On the basis of these observations and the chemical shifts of these resonances, the signals at 6.12, 2.78, 2.48, 4.70, 4.27 and 4.19 ppm were assigned to H1', H2', H2'', H3', H4' and H5'/H5'' resonances of 3'-G of conformer **I**, respectively (Figures S1-S2, Table 1).

The third H8 signal (8.28 ppm) showed NOE cross-peaks to signals at 2.48, 6.24 and 4.19 ppm. An NOE and COSY cross-peaks between the signal at 2.48 ppm and a signal at 6.24 ppm was also found (Figures 3-4, Table 1). The signal at 2.48 ppm showed NOE and COSY cross-peaks to a resonance at 2.78 ppm, and NOE cross-peaks to signals at 4.92 and 4.19 ppm. The signal at 6.24 ppm showed NOE and COSY cross-peaks to a resonance at 2.52 ppm, and NOE cross-peaks to signals at 4.92 and 4.19 ppm. On the basis of these observations and the chemical shifts of these resonances, the signals at 6.24, 2.78, 2.48, 4.92 and 4.19 ppm were assigned to H1', H2', H2'', H3' and H4' resonances of 5'-G of conformer **II**, respectively (Figures 3-4, Table 1).

The fourth H8 signal (8.34 ppm) showed NOE cross-peaks to signals at 2.48, 6.13 and 4.18 ppm. An NOE and COSY cross-peaks between the signal at 2.48 ppm and a signal at 6.13 ppm was also found (Figures 3-4, Table 1). The signal at 2.52 ppm showed NOE and COSY cross-peaks to a resonance at 2.78 ppm, and NOE cross-peaks to signals at 4.66 and 4.18 ppm. The signal at 6.13 ppm showed NOE and COSY cross-peaks to a resonance at 2.48 ppm, and NOE cross-peaks to signals at 4.66 and 4.18 ppm. On the basis of these observations and the chemical shifts of these resonances, the signals at 6.13, 2.78, 2.48, 4.66 and 4.18 ppm were assigned to H1', H2', H2'', H3' and H4' resonances of 3'-G of conformer **II**, respectively (Figures S1-S2, Table 1).

The binding of **1'** via GN7 is also confirmed by the ¹H chemical shifts of Ho, Hm and Hp protons of coordinated arene A in Ru₂-GpG. For example, in complexes **1'**-9EtG, **1'**-Guo and **1'**-GMP,⁴ the Ho or Hm resonances shift slightly to low-field from 0.09 ppm to 0.15 ppm, or from 0.31 to 0.37 ppm, respectively; the Hp resonances shift to high-field by from -0.19 ppm to -0.25 ppm. In present case, similar chemical shifts for Ho, Hm and Hp resonances of **1'a**, **1'b** and **1'c** are observed: Ho or Hm resonances shift slightly to low-field from +0.05 ppm to 0.19 ppm, or from +0.46 ppm to 0.52 ppm, respectively, the Hp resonances shift to high-field by -0.42 ppm. For **1'd**, the Hm resonance shifts slightly to low-field (+0.17 ppm) and Hp resonance to high-field by -0.49 ppm, but Ho resonance shifts slightly to high-field (-0.07 ppm).

Guanine bases in Ru₂-GpG. Figure S1 shows that there are four sets of signals for guanine bases, indicating that there are two conformers (**I** and **II**) for the di-ruthenated adduct Ru₂-GpG. For 5'-G(**I**), a large low-field shift of the H8 resonance was observed, as was also the case for H2', H2'' protons, relative to free d(GpG) (Figure 4 and Table 1). The H3' and H5'/H5'' resonances were shifted slightly to low-field. For 3'-G(**I**), a large low-field shift of the H8 resonance was observed, relative to free d(GpG) (Table 1). The H4' and H5'/H5'' resonances were shifted slightly to low-field, however, the resonance H1' was shifted slightly to high field. For 5'-G(**II**), a large low-field shift of the H8 resonance was observed, relative to free d(GpG) (Table 1); the H2', H2'', H3' resonances were shifted to low-field; but the resonance H1' was shifted to high field. For 3'-G(**II**), a large low-field shift of the H8 resonance was observed, relative to free d(GpG) (Table 1), while the resonances H1' and H3' were shifted to high field.

Determination of binding sites by NMR. Selective binding to N7 of the G residues of d(GpG) was evident from the [¹H, ¹H] NOESY NMR spectrum and confirmed by ¹H NMR chemical shift changes (Figure 4, and Tables 2 and 3). NOE connectivities between ruthenated GH8 and 1'-NHu or 1'-NHd were observed in the [¹H, ¹H] NOESY NMR spectra for major conformers **I** and minor conformer **II** of Ru₂-GpG. Binding of **1'** to 9EtG, Guo and 5'-GMP *via* N7 causes a low-field shift of H8 resonance of +0.40 to +0.51 ppm.^{4,13} Binding of **1'** to 6-mer duplex DNA d(CGGCCG)₂ or 14-mer duplex d(ATACATGGTACATA)•d(TCTGTACCATGTCT) *via* N7 causes low-field shifts of the H8 resonance up to +0.40 or +0.79 ppm, respectively.¹⁴⁻¹⁵ Similar low-field shifts were observed for the GH8 resonances in Ru₂-GpG adduct, and allow assignment of the binding sites as 5'-G or 3'-G ($\Delta\delta$ H8 +0.46, 0.41, 0.52, or 0.30 ppm) in major conformer **I** and minor conformer **II**, respectively (Figures S1 and 4, Table 1).

The ³¹P chemical shift changes were also consistent with ruthenation at N7 of G residues of d(GpG) by **1'**. Binding of **1'** to the phosphate of 5'-GMP^{4,13} causes a low-field shift of the ³¹P NMR resonance by up to +5.11 ppm. However, the binding of **1'** to N7 of 5'-GMP,^{4,13} ³¹P NMR shifts less than ± 2 ppm. In the present case, the most affected ³¹P NMR signal assigned to the phosphate group for conformer **I** of Ru₂-GpG shifts to high-field by -1.73 ppm, and less affected ³¹P NMR signal assigned to the phosphate group

for conformer **II** of Ru₂-GpG shifts to high-field by -0.64 ppm (Figures S3 and S4).

Bound fragments 1'a-1'd. Figure S1 shows 600 MHz 1D ¹H NMR spectra of HPLC-purified diruthenated [Ru₂d(GpG)] in both 90% H₂O/10% D₂O (Figure S1A) and in 100% D₂O solutions (Figure S1B). It was notable that broad peaks around 6.55 ppm were observed for the 90% H₂O/10% D₂O solution (Figure S1B), but these disappeared after this sample was lyophilized repeatedly from 99.9% D₂O and re-dissolved in 99.99% D₂O (Figure S1B). This finding together with the 2D [¹H, ¹⁵N] HSQC NMR data (Figure S2) and NOESY connectivities in 90% H₂O/10% D₂O (not shown) observed between these peaks and Hm and Hp resonances or NHd resonances (Tables 2 and S1), confirmed that these resonances were NHu resonances of bound fragment $\{(\eta^6\text{-bip})\text{Ru}(\text{en})\}^{2+}$ of **1'a-1'd**. 2D [¹H, ¹⁵N] HSQC NMR experiments allowed assignment of NMR peaks specifically for the $\{(\eta^6\text{-biphenyl})\text{Ru}(\text{en})\}^{2+}$ (¹⁵N-**1**, ¹⁵N-en labelled complex **1**) fragment. These are commonly difficult to resolve in normal ¹H NMR experiments. Three major new peaks were detected by 2D [¹H, ¹⁵N] HSQC NMR analysis of the di-ruthenated Ru₂-GpG adduct with ¹⁵N-**1** at 298 K in 90% H₂O/10% D₂O (Figure S2). Four pairs of NOESY connectivities were observed between NHu and NHd resonances in the 90% H₂O/10% D₂O. Four sets of signals for the non-coordinated phenyl ring B and coordinated phenyl ring A of bound fragment $\{(\eta^6\text{-bip})\text{Ru}(\text{en})\}^{2+}$ (**1'a-1'd**) were detected in the 2D COSY and NOESY NMR spectra. This can be seen for example in Figures 3 and 4 and Table 2. One set of almost un-shifted signals for en CH₂ (2.45 ppm) for **1'a-1'c** was detected.

3'-G and 5'-G bases in Ru₂-GpG. Non-equivalent 3'-G and 5'-G bases of d(GpG) have been observed for d(GpG) adducts of di-functional *cis*-DDP⁵ and its analogs, dinuclear platinum complexes,⁶ dirhodium or di-functional Ru(III) complexes.⁷ The H8 NMR signal separations in d(GpG) adducts are related to their conformations. For example, larger H8 signal separations are found in head-to-head (HH) conformations, and smaller H8 signal separations are observed for head-to-tail (HT) conformations. den Hartog et al⁵ reported that the GH8 signal separation is 0.305 ppm for a HH conformer of the *cis*-DDP-d(GpG) adduct, and Marzilli et al⁸⁻¹⁰ have shown that the GH8 signal separations for HH1 conformers (up to 1.23 ppm) is much larger than that of ΔHT1 conformers (0.07 ppm) for adduct (S,R,R,S)-BipPt(d(GpG)) (Bip = 2,2'-

bipiperidine) or Me₂ppzPt(d(GpG)) (Me₂ppz = N,N'-dimethylpiperazine). For the HH1 or HH2 conformers of the d(GpG) adduct with Rh₂(OAc)₂¹¹ (OAc = CH₃CO₂), Chifotides et al.¹² have shown that the GH8 signal separations are 0.22 or 0.34 ppm, respectively. The flexibility of the d(GpG) adducts may enhance the equivalence of the 5'-G and 3'-G guanine bases in "stepped head-to-head" conformers, for example, Farrell et al.⁶ have shown that GH8 signal separations are smaller (from 0.03 to 0.37 ppm) for 1,1/t,t-d(GpG) adducts formed by a series of dinuclear platinum complexes [*trans*-PtCl(NH₃)₂]₂{μ-H₂N(CH₂)_nNH₂}]²⁺ (1,1/t,t, n = 2-6), and the smallest H8 signal separation is observed for the 1,1/t,t-d(GpG) adduct with the longest diamine chain length (n = 6). On the other hand, the d(GpG) adduct with a ruthenium(III) complex⁷ also shows a small GH8 signal separation, for example, the two GH8 protons of the d(GpG) adduct with *trans*-RuCl₂(DMSO)₄ appear at 8.659 or 8.753 ppm, the H8 signal separations is only 0.094 ppm.

In the present work, two distinct monofunctional Ru motifs bind to their respective guanine base separately, and di-ruthenated d(GpG) adduct Ru₂-GpG is formed in a quite different way in comparison to that of the *cis*-DDP and its analogs, dirhodium complexes¹¹⁻¹² and RuCl₂(DMSO)₄⁷ which form 1, 2 cross-link binding mode with d(GpG), for dinuclear platinum complexes, the monofunctional Pt motifs are connected by linker chains of different lengths.⁶ The relatively small GH8 signal separations (0.23 or 0.06 ppm) for the major conformer **I** or minor conformer **II** of di-ruthenated adduct Ru₂-GpG, respectively. These obviously different H8 NMR signal separations may imply that there are structural difference between major conformer **I** and minor conformer **II** of the di-ruthenated adduct Ru₂-GpG.

Connectivities between d(GpG) and bound fragments 1'a-1'd. NOE cross-peaks were found between protons of 5'-G(**I**)-and **1'a** (Figure 4 and Table 3), and between protons of 3'-G(**I**) and **1'b** (Figure 4 and Table 3), respectively. NOE cross-peaks were also observed between protons of 5'-G(**II**) and **1'c** (Figure 4 and Table 4), between protons of 3'-G(**II**) and **1'd** (Figure 4 and Table 4), respectively. Unusual NOE connectivities were observed between arene protons of **1'b** and **1'a** in major conformer **I** of Ru₂-GpG (Figure 4 and Table 5). For example, weak NOESY cross-peaks were found between **1'a**-Ho' and **1'b**-Hp protons, **1'a**-Hm' and **1'b**-Hm protons, very weak NOE cross-peaks were observed between **1'a**-Hp and **1'b**-Ho'

protons, between **1'a**-Hp and **1'b**-Hp' protons, and between **1'a**-Hp and **1'b**-Hm' protons. Weak NOE cross-peaks were also observed between **1'a**-Hm and 3'-G(**I**)-H5'/H5'' protons. However, no such NOE cross-peaks were observed for minor conformer **II** of Ru₂-GpG.

Table S1. Chemical shifts of en-NH protons of **1'** the various Ru-arene adducts.^a

Ru-arene adducts	δ NHu	δ NHd
[Ru ₂ d(GpG)] I (major)	6.55(a)	4.34(a)
[Ru ₂ d(GpG)] II (minor)	6.58(b)	4.31(b)
	6.58(c)	4.34(c)
	6.57(d)	4.00(d)
III -Ru-G18i	6.60 (a)	4.48 (a)
III -Ru-G18n	6.51 (b)	4.40 (b)
III -Ru-G7	6.51 (b)	4.70 (b)
III -Ru-G8	6.56 (c)	4.94 (c)
and/or III -Ru-G25 ^b	6.47 (d)	4.84 (d)
1	6.19	4.14
1 -H ₂ O	6.04	4.02
1' -9EtG ^c	6.53	nd ^d
1' -GMP ^{c,e}	6.32	5.26
	6.36	5.11

^a The assignment of en-NH₂ protons as 'u' or 'd' (Scheme 1) is based on previous work (Chen, H.; Parkinson, J. A.; Parsons, S.; Coxall, R. A.; Gould, R. O.; Sadler, P. J.; *J. Am. Chem. Soc.*, **2002**, *124*, 3064) and the pairs (labelled a-d) are identified on the basis of NOESY NHu-NHd cross-peaks in the mixture of three diruthenated GpG adducts in the 90%-H₂O/10%D₂O experiments. A total of 8 different pairs of NHu and NHd protons will be present but only four cross-peaks were identified as a consequence of overlap, resonances too broad to observe and/or suppression of NHd resonances close to the ¹H₂O resonance. The labels (a), (b), (c) and (d) distinguish cross-peaks for intramolecular NOEs between NHu and H8 protons observed for different conformers of adduct (see Tables 3-5).

^b **III** = d(ATACATGGTACATA) • d(TATGTACCATGTAT). Liu, H. K.; Berners-Price, S. J.; Wang, F.; Parkinson, J. A.; Xu, J.; Bella, J.; Sadler, P. J.; *Angew. Chem. Int. Ed.*, **2006**, *45*, 8153-8156.^c Chen, H.; Parkinson, J. A.; Parsons, S.; Coxall, R. A.; Gould, R. O.; Sadler, P. J.; *J. Am. Chem. Soc.*, **2002**, *124*, 3064. ^dToo broad to observe. ^eMeasured at 310 K.

Table S2. Negative ions detected by HPLC-ESI-MS for products from reaction of [(η^6 -biphenyl)RuCl(en)]⁺ (**1**) with d(GpG).

Reaction	RT ^a [min]	Obs (Calcd) ^b <i>m/z</i>	Ions
1Ru:1d(GpG)	3.96	595.1 (595.4)	{d(GpG)} ⁻
	6.73	350.8 (350.8)	{ 1' } ⁺
	9.77	913.1(913.2)	{ 1' + d(GpG) - Cl} ⁺
	12.78	314.8 (315.3)	{ 1' - Cl} ⁺
2Ru:1d(GpG)	6.73	350.8 (350.8)	{ 1' } ⁺
	9.77	913.1(913.2)	{ 1' + d(GpG) - Cl} ⁺
	12.78	314.8 (315.3)	{ 1' - Cl} ⁺
	16.48	672.6(672.1)	{ 1' ₂ + d(GpG) + CF ₃ CO ₂ - 2Cl} ²⁺
5Ru:1d(GpG)	6.73	350.8 (350.8)	{ 1' } ⁺
	9.77	913.1(913.2)	{ 1' - d(GpG)} ⁺
	12.78	314.8 (315.3)	{ 1' - Cl} ⁺
	16.48	672.6(672.1)	{ 1' ₂ + d(GpG) + CF ₃ CO ₂ - 2Cl} ²⁺

^a RT is the HPLC retention time (Figure 2). ^b Observed (Obs) and calculated (Calcd) mass-to-charge ratios for the observed ions. For chemical structures, see Figure 1.

Table S3. Intramolecular NOEs between protons of **1'c** and **1'd** and d(GpG) in conformer **II** (minor).^a

Base	Proton	[Ru ₂ -d(GpG)] II (minor)
5'-G(II)	H8	1'c -Ho'(w, broad), 1'c -Ho(w, broad), 1'c -Hm(vw), H2'' (m, broad),
	8.28	H1'(m,broad), ^c H4' (vw)
	H1'	1'c -Ho'(w, broad), H8(m, broad), H2''(w, broad), H4'(vw, broad)
	6.24	
	H2''	H1'(w, broad), ^c 1'c -Ho'(w, broad), 1'c -Ho(w), ^c H8(s, broad), H4'(vw, broad),
	2.48	H3'(vw, broad)
	H3'	H2''(m, broad), H4'(w, broad)
	4.92	
H4'	H2'' (w)	
4.19		
3'-G(II)	H8	1'd -Ho'(vw), H1'(w, broad), ^d H2''(w, broad), H4'(vw), NHu(vvw) ^b
	8.34	
	H1'	H8(vw, broad), H4'(vw), H2''(m, broad), 1'd -Ho'(w), ^d H3'(w, broad)
	6.13	
	H2''	H1'(m, broad), ^d 1'd -Ho' (w), ^d H8(w, broad), H3'(m, broad), H4'(w, broad)
	2.48	
	H3'	H1'(w, broad), ^d H2''(m, broad), H4'(w, broad)
	4.66	
H4'	H2''(m, broad), H1'(m, broad), ^d H8(vw, broad)	
4.18		

^a For atom labels see Scheme 1.

^b Assignment was made only in 90%²H₂O-10%²D₂O experiment.

^c 5'-G(**II**)-H1' and **1'b**-Ho are coincident.

^d 3'-G(**II**)-H1' and **1'd**-Ho are coincident. s = strong, m = medium, w = weak, vw = very weak.

Table S4. Intramolecular NOEs and distances in model **A** (see Fig. 5A-B) between arene protons of **1'a** and **1'b** in major conformer **I**.^a

Intramolecular NOEs	Distance (Å) in model A	NOE intensity
1'a -Ho'/ 1'b -Hp	4.91,5.37	w ^b
1'a -Hm'/ 1'b -Hm ^c	3.53,4.03	w
1'a -Hp/ 1'b -Ho'	4.32, 5.45	vw
1'a -Hp/ 1'b -Hp'	3.66	vw
1'a -Hp/ 1'b -Hm'	3.41,4.73	vw
1'a -Hm/3'-G(I)-H5'/H5''	3.58, 4.38	w

^a For atom labels see Scheme 1. ^b w = weak, vw = very weak. ^cthis cross-peak is overlapped with **1'b**-Ho-Ho'.

Table S5. Distances between protons of d(GpG) and **1'a** or **1'b** in model **A**.

base	Proton of base	Proton of 1'	Distance (Å)	NOE intensity
5'-G	H8	1'a -Ho'	2.99	w-m
	H8	1'a -Ho	2.72	m-s
	H8	1'a -NHu	2.61	S
	H8	1'a -Hm	3.34	w
	H2''	1'a -Ho	5.52	w
3'-G	H8	1'b -Ho'	3.46	m
	H8	1'b -Ho	3.12	w-m
	H8	1'b -NHu	3.74	vw
	H8	1'b -Hm	3.59	w-m
	H1'	1'b -Ho'	4.91	w
	H2''	1'b -Ho'	4.18	w
	H2''	1'b -Ho	4.13	w

s = strong, m = medium, w = weak, vw = very weak, vvw = very very weak.

Table S6. Distances between protons of d(GpG) and **1'c** or **1'd** in model **C** (see Fig 5D).

Base	Proton of base	Proton of 1'	Distance (Å)	NOE intensity
5'-G	H8	1'c -Ho	5.24	w
	H8	1'c -Hm	3.64,4.40	vw
3'-G	H1'	1'd -Ho'	5.33	w
	H2''	1'd -Ho'	3.98, 4.47	w

w = weak, vw = very weak.

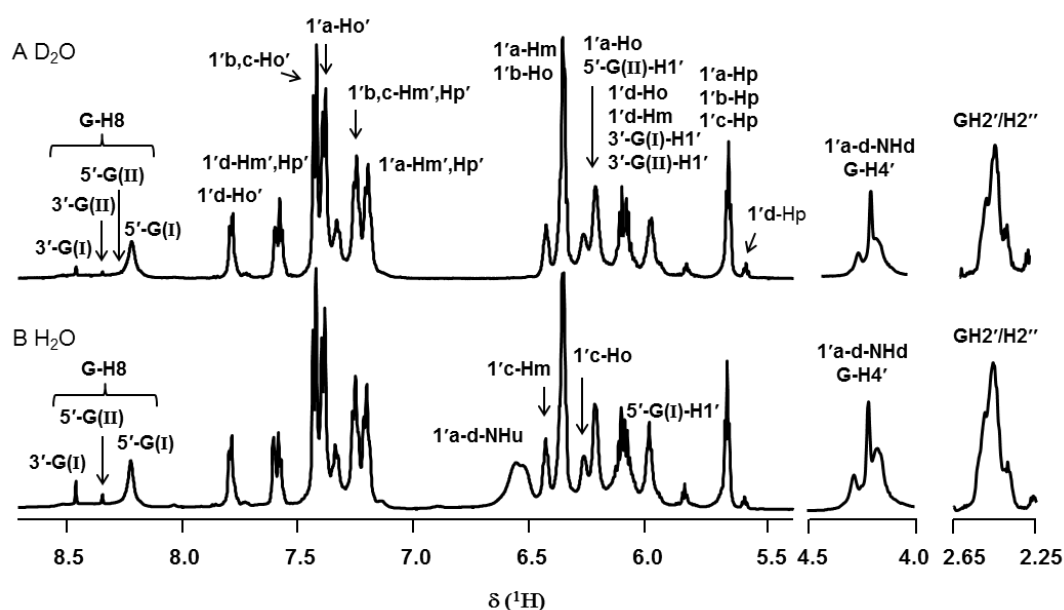


Figure S1. 600 MHz ^1H NMR spectra of the HPLC-separated di-ruthenated d(GpG) adducts $[\text{Ru}_2\text{-d(GpG)}]$ in both 100% D_2O (A) and 90% $\text{H}_2\text{O}/10\%$ D_2O solutions (B) at 283 K, 2.34 mM in 0.1 M NaClO_4 , pH 7.0. Assignments of proton resonances for both d(GpG) and $\mathbf{1'a-1'd}$, ($\mathbf{1'a-1'd}$ are the bound fragment $\mathbf{1'}$, $\{(\eta^6\text{-biphenyl})\text{Ru}(\text{en})\}^{2+}$), are indicated. The assignments of peaks for bases $\mathbf{5'-G(I)}$ and $\mathbf{3'-G(I)}$ (major conformer **I**), $\mathbf{5'-G(II)}$ and $\mathbf{3'-G(II)}$ (minor conformer **II**), bound fragments $\mathbf{1'a}$ to $\mathbf{1'd}$ are based on 2D DQF-COSY and NOESY experiments (shown in Figures 3 and 4, see also Tables 1, 2 and 3).

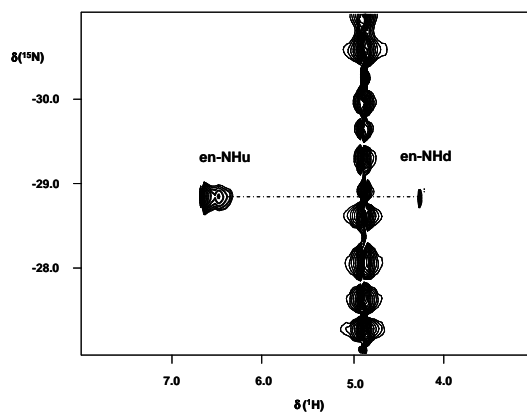


Figure S2. 2D [^1H , ^{15}N] HSQC NMR spectra of di-ruthenated [$\text{Ru}_2\text{-d(GpG)}$] (2.34 mM, 0.1 M NaClO_4 at 298 K, pH 7.0) in 90% $\text{H}_2\text{O}/10\%$ D_2O . Peaks at 6.55/-28.62 and 6.40/-28.62 ppm are assignable to en-NHu resonances, at 4.32/-28.62 ppm to en-NHd resonances of [$\text{Ru}_2\text{-d(GpG)}$] ($\text{Ru} = \{(\eta^6\text{-biphenyl})\text{Ru}(\text{en})\}^{2+}$ (**1'**)). For atom labels, see Figure 1.

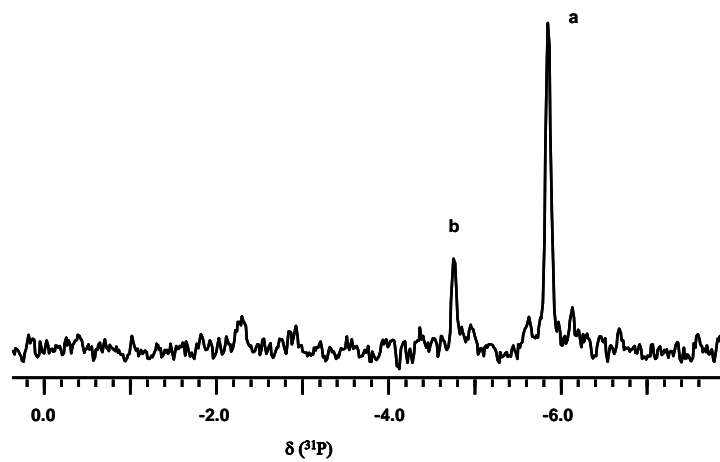


Figure S3. 1D ^{31}P NMR spectrum of di-ruthenated d(GpG) adduct at 298 K in 10% $\text{D}_2\text{O}/90\%$ H_2O , showing two ^{31}P peaks at -5.83 (a) and -4.74 ppm (b). For atom and base labels, see Figure 1 and Table 1.

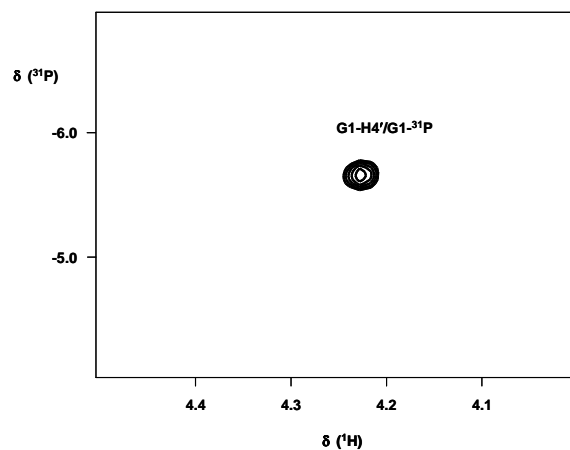


Figure S4. 2D [^1H , ^{31}P] HSQC NMR spectrum of $\text{Ru}_2\text{-d(GpG)}$ in 90% H_2O /10% D_2O at 298 K. The peak at 4.23/-5.83 ppm is assignable to the 5'-G(I)H4'/5'-G(I)- ^{31}P connectivity. For atom labels, see Figure 1 and Scheme 1.

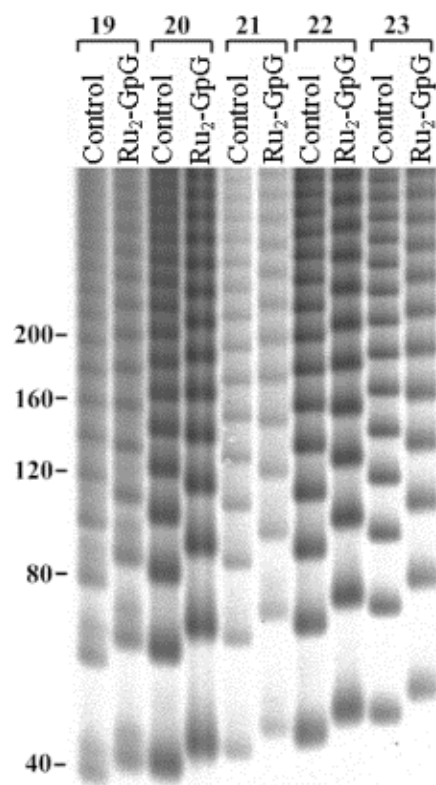


Figure S5. Autoradiogram of the ligation products of double-stranded oligonucleotides TGGT (19-23) nonmodified or containing two monofunctional adducts of Ru-biphenyl. The ligation products were separated on an 8% PAA gel. Lanes: Control, nonmodified duplexes; Ru₂-GpG, duplexes containing two adjacent Ru-biphenyl adducts.

TGGT (19)
1 2 3 4 5 6 7 8 9 10 11 12 13 14 15 16 17 18 19
5' - CCTCTCCTTGGTCTCCTTC - 3' GG
3' - GAGAGGAACCAGAGGAAGG - 5' CC
19 18 17 16 15 14 13 12 11 10 9 8 7 6 5 4 3 2 1

TGGT (20)
5' - CCTCTCCTTGGTCTCCTTCT - 3'
3' - GAGAGGAACCAGAGGAAGAG - 5'

TGGT (21)
5' - CCTCTCCTTGGTCTCCTTCTC - 3'
3' - GAGAGGAACCAGAGGAAGAGG - 5'

TGGT (22)
5' - CCTCTCCTTGGTCTCCTTCTCT - 3'
3' - GAGAGGAACCAGAGGAAGAGAG - 5'

TGGT (23)
5' - CCTCTCCTTGGTCTCCTTCTCTC - 3'
3' - GAGAGGAACCAGAGGAAGAGAGG - 5'

Figure S6. Sequences of the synthetic oligodeoxyribonucleotide duplexes used in this study and their abbreviations.

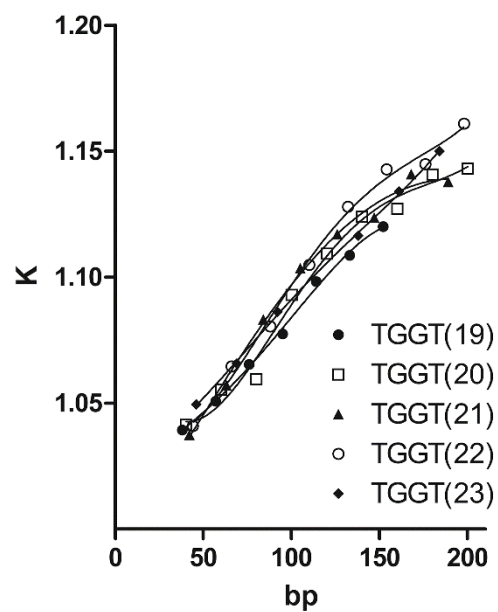


Figure S7. Plots showing the relative mobility K versus sequence length for the oligomers (TGGT)/(ACCA) (19-23) containing Ru-biphenyl adducts.

References

1. H. K. Liu, J. A. Parkinson, F. Wang, J. Bella, P. J. Sadler, *Chem. Sci.*, 2010, **1**, 258-270.
2. H.-K. Liu and P. J. Sadler, In *Interactions of metallodrugs with DNA in NMR of Biomolecules: Towards Mechanistic Systems Biology*. I. Bertini, K. McGreevy (Ed), Wiley-VCH, 2012, Chapter 16, pp 282-296.
3. H. Chen, J. A. Parkinson, R. E. Morris, P. J. Sadler, *J. Am. Chem. Soc.*, 2003, **125**, 173-186.
4. H. Chen, J. A. Parkinson, S. Parsons, R. A. Coxall, R. O. Gould, P. J. Sadler, *J. Am. Chem. Soc.*, 2002, **124**, 3064-3082.
5. J. H. J. den Hartog, C. Altona, J. C. Chottard, J. P. Girault, J.-Y. Lallemand, F. A. A. M. de Leeuw, A. T. M. Marcelis, and J. Reedijk, *Nucleic Acids Res.*, 1982, **10**, 4715.
6. Y. Qu, M. J. Bloemink, J. Reedijk, T. W. Hambley, N. Farrell, *J. Am. Chem. Soc.*, 1996, **118**, 9307-9313.
7. G. Esposito, S. Cauci, F. Fogolari, E. Alessio, M. Scocchi, F. Quadrifoglio, P. Viglino, *Biochem.*, 1992, **31**, 7094-7103.
8. S. T. Sullivan, A. Ciccarese, F. P. Fanizzi, L. G. Marzilli, 2001, *J. Am. Chem. Soc.*, 2001, **123**, 9345-9355 and references therein.
9. K. M. Williams, L. Cerasino, G. Natile, L. G. Marzilli, *J. Am. Chem. Soc.*, 2000, **122**, 8021-8030.
10. L. G. Marzilli, S. O. Ano, F. P. Intini, G. Natile, *J. Am. Chem. Soc.*, 1999, **121**, 9133-9142.
11. H. T. Chifotides, K. R. Dunbar, *Chem. Eur. J.*, 2006, **12**, 6458.
12. H. T. Chifotides, K. M. Koshlap, L. M. Perez, K. R. Dunbar, *J. Am. Chem. Soc.*, 2003, **125**, 10703.
13. H. Chen, J. A. Parkinson, R. E. Morris, P. J. Sadler, *J. Am. Chem. Soc.*, 2003, **125**, 173-186.
14. H. K. Liu, S. J. Berners-Price, F. Wang, J. A. Parkinson, J. Xu, J. Bella, P. J. Sadler, *Angew. Chem. Int. Ed.*, 2006, **45**, 8153-8156.
15. H. K. Liu, F. Wang, J. A. Parkinson, J. Bella, P. J. Sadler, *Chem. Eur. J.*, 2006, **12**, 6151-6165.